RSC Advances

ROYAL SOCIETY OF CHEMISTRY

www.rsc.org/advances

Novel photochromic and electrochromic diarylethenes bearing triphenylamine units

Huiyi Jin[a,b], Jianhua Tian[a,b], Shirong Wang*[a,b], Tingfeng Tan*[c], Yin Xiao[a,b] and Xianggao Li[a,b]

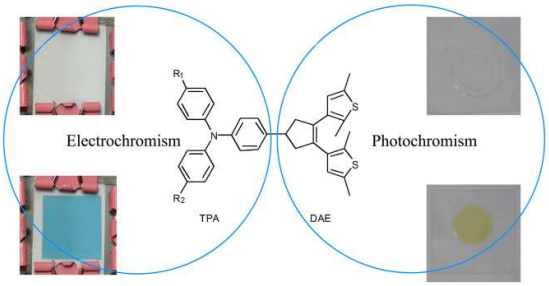

Novel diarylethenes containing triphenylamine units have been synthesized and characterized, which were possessed of both photochromic and electrochromic properties.

Novel photochromic and electrochromic diarylethenes bearing triphenylamine units

Huiyi Jin[a,b], Jianhua Tian[a,b], Shirong Wang*[a,b], Tingfeng Tan*[c], Yin Xiao[a,b] and Xianggao Li[a,b]

[a]School of Chemical Engineering and Technology, Tianjin University, Tianjin 300072, P.R. China, E-mail: wangshirong@tju.edu.cn

[b]Collaborative Innovation Center of Chemical Science and Engineering, Tianjin 300072, P.R. China

[c]School of Science, Tianjin Chengjian University, Tianjin 300384, P.R. China, E-mail: tantingfeng@126.com

Abstract: Six novel photochromic and electrochromic diarylethenes containing triphenylamine units were synthesized by McMurry reaction. The properties of photochromism, electrochromism, fluorescence and electrochemistry were investigated in detail. The results showed that these compounds exhibited reversible photochromism, changing from colorless to yellow after irradiation with 302 nm UV light both in solution and in PMMA amorphous film. When arriving at the photostationary state, the fluorescent intensity was quenched to about 40%. In the cyclic voltammetry curves, there were a reversible redox couple and one or two irreversible oxidation peaks. The potential of reversible oxidation peak is adopted as the excitation voltage of electrochromism. The electrochromic devices could be simulated with an equivalent circuit, R(CR)(CR), by electrochemical impedance spectroscopy, and realized the transformation between colorless and blue, which required 8.6 to 12.1 s for color switching and 8.9 to 12.8 s for bleaching. The reflectance minima of these compounds are in the range from 709.7 to 781.7 nm after coloring. The results showed that diarylethenes containing triphenylamine units were possessed of both photochromic and electrochromic properties.

Keywords: photochromism; electrochromism; diarylethene; triphenylamine; electrochemistry

1. Introduction

Photochromism is the reversible transformation of a chemical species between two forms with different absorption spectra, which caused by alternating irradiation with UV and visible light.[1] Over the past 40 years, photochromic compounds have attracted more attention because of the potential application in high-density optical recording materials, photo switches and light-controlled molecular machines.[2]

Among various types of photochromic compounds, diarylethene (DAE) derivatives with heterocyclic aryl rings are the most promising candidates for photoelectronic applications because of the notable fatigue resistance, high thermal stability, and rapid response.[3] Tian et al have successfully developed some new photochromic materials with ions recognition ability composed of *N*-butyl-1,8-naphthalimide and piperazine, which exhibited multi-responses to UV irradiation, proton and copper (II) ions.[4] A novel dimethylaminophenyl thiazole diarylethene that display some acid-gated photochromism and photomodulation properties were investigated by

Coudret et al.[5] Akita et al have intensively explored a series of DAE derivatives with a directly σ-bonded, redox-active organometallic attachment, which showed photochromic and electrochromic behavior.[6] Hence, current research interest is focused on the introduction of function groups to obtain novel photochromic materials with more excellent properties.[7]

Electrochromism is the phenomenon displayed by some materials of reversibly changing optical color when a suitable potential is applied, due to some of the visible light being absorbed by the material itself,[8] which was used in the field of smart windows,[9] mirrors of vehicles,[10] electronic paper,[11] and so on. Currently, triphenylamine (TPA) derivatives have been extensively used as a kind of good electrochromic material as it easily oxidizes to form radical cation with a noticeable change of coloration.[12] Electrochromic properties of aromatic polyamides with TPA unites have been sufficiently studied by Liou et al.[13] However, there are few reports about DAE modified by TPA units, which might possess photochromic and electrochromic properties simultaneously.

In the present work, six novel diarylethenes bearing triphenylamine units (TPA-DAEs) (**1a~1f**) were designed and synthesized (Scheme 1). Photochromism, fluorescence, electrochemistry and electrochromism of the compounds have been studied in detail.

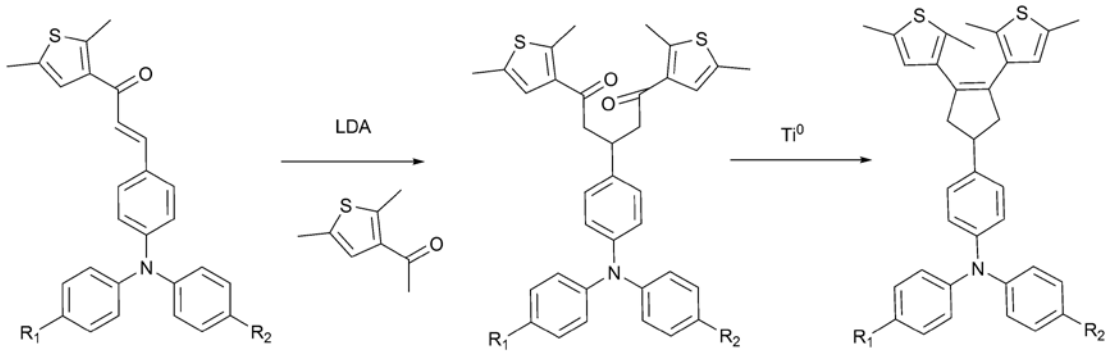

Scheme 1. Synthetic route for the target compounds.

2. Experimental Section

2.1. General

All the chemical reagents and solvents, unless otherwise stated, were used as received from commercial sources without further purification. Tetrahydrofuran (THF) was refluxed with sodium and diphenylketone, which was fractionally distilled while the green color of the disodium salt of diphenylketone was well established. Compounds **2a~2f** were prepared by our group. Silica gel 60 (300~400 mesh) was used for column chromatography. NMR spectra (^{1}H at 400 MHz, ^{13}C at 100 MHz) were obtained in $CDCl_3$ using an AVANCE III spectrometer with tetramethylsilane (TMS) as the internal standard. Mass spectra were recorded on a LCQ Deca XP MAX mass

spectrometer. Elemental analysis was performed on a Vario Micro cube elemental analyzer. Thermogravimetric analysis (TG) was conducted with a SEIKO TG/DTA6300. Cyclic voltammetry experiment in dilute dichloromethane solution was performed on a CHI660E impedance measurement unit. The absorption spectra were measured using PE LAMBDA35 spectrometer. Photoirradiation was carried out using a ZF-90 ultraviolet perspective reverberate analysis cabinet and a T815 blue light flashlight. Emission spectra were measured using F-7000 spectrometer.

2.2. Preparation of pentane-1,5-dione derivatives

To a stirred solution of 3-acetyl-2,5-dimethylthiophene (5.5 mmol) in dry THF (20 mL) was added lithium diisopropylamide (LDA) (3 mL, 2.0 M solution in THF) slowly at -25°C in an atmosphere of argon. After stirred for 10 min, a solution of corresponding chalcone (5 mmol) in dry THF (15 mL) was added by dropwise into the reaction mixture. The resulting mixture was stirred for 15 min at -25°C and allowed to come to room temperature over 2 h. The reaction mixture was quenched with ice water, neutralized by adding 1 N hydrochloric acid and extracted with dichloromethane. The organic phase was washed with brine, dried over magnesium sulfate, filtered, concentrated and separated by flash column chromatography to give corresponding pentane-1,5-dione.

1,5-Bis(2,5-dimethylthiophen-3-yl)-3-[4-(diphenylamino)phenyl]pentane-1,5-dione (**3a**). 1.88 g, yellow solid, yield: 67%, m.p. 44-45°C. ^{1}H NMR (400 MHz, $CDCl_3$) δ: (ppm) 7.21 (t, J = 7.7 Hz, 4H), 7.09 (d, J = 8.3 Hz, 2H), 7.06-6.93 (m, 10H), 3.88 (p, J = 6.9 Hz, 1H), 3.15 (ddd, J = 42.2, 16.1, 7.0 Hz, 4H), 2.58 (s, 6H), 2.39 (s, 6H); ^{13}C NMR (100 MHz, $CDCl_3$) δ: (ppm) 194.91, 147.86, 147.26, 138.47, 135.73, 135.05, 129.13, 128.23, 126.02, 124.29, 123.97, 122.49, 47.99, 36.64, 15.91, 15.01, 1.03.

1,5-Bis(2,5-dimethylthiophen-3-yl)-3-{4-[phenyl(4-methylphenyl)amino]phenyl}pentane-1,5-dione (**3b**). 2.07 g, yellow solid, yield: 72%, m.p. 43-44°C. ^{1}H NMR (400 MHz, $CDCl_3$) δ: (ppm) 7.22 (t, J = 7.8 Hz, 2H), 7.14-6.96 (m, 13H), 3.92 (p, J = 6.9 Hz, 1H), 3.19 (ddd, J = 42.2, 16.1, 7.1 Hz, 4H), 2.62 (s, 6H), 2.43 (s, 6H), 2.34 (s, 3H); ^{13}C NMR (100 MHz, $CDCl_3$) δ: (ppm) 194.94, 148.07, 147.25, 146.25, 145.27, 138.03, 135.75, 135.05, 132.56, 129.87, 129.06, 128.15, 126.05, 124.78, 123.76, 123.38, 122.03, 48.03, 36.63, 20.84, 15.94, 15.03.

1,5-Bis(2,5-dimethylthiophen-3-yl)-3-{4-[bis(4-methylphenyl)amino]phenyl}pentane-1,5-dione (**3c**). 1.88 g, yellow solid, yield: 66%, m.p. 56-58°C. ^{1}H NMR (400 MHz, $CDCl_3$) δ: (ppm) 7.10-6.93 (m, 14H), 3.90 (p, J = 6.8 Hz, 1H), 3.18 (ddd, J = 41.4, 16.1, 7.0 Hz, 4H), 2.62 (s, 6H), 2.43 (s, 6H), 2.33 (s, 6H); ^{13}C NMR (100 MHz, $CDCl_3$) δ: (ppm) 194.99, 147.23, 146.48, 145.48, 137.47, 135.75, 135.02, 132.07, 129.76, 128.03, 126.06, 124.25, 123.11, 48.05, 36.61, 20.80, 15.93, 15.02.

1,5-Bis(2,5-dimethylthiophen-3-yl)-3-{4-[phenyl(4-methoxyphenyl)amino]phenyl}pentane-1,5-dione (**3d**). 2.26 g, yellow solid, yield: 76%. m.p. 48-50°C. ^{1}H NMR (400 MHz, $CDCl_3$) δ: (ppm) 7.21 (t, J = 7.8 Hz, 2H), 7.11-6.93(m, 11H), 6.84 (d, J = 8.8 Hz, 2H), 3.90 (p, J = 6.9 Hz, 1H), 3.82 (s, 3H), 3.17 (ddd, J = 41.4, 16.2, 7.0 Hz, 4H), 2.61 (s, 6H), 2.42 (s, 6H); ^{13}C NMR (100 MHz, $CDCl_3$) δ: (ppm) 194.94, 156.07, 148.23, 147.24, 146.38,

140.79, 137.64, 135.74, 135.03, 128.99, 128.08, 127.18, 126.04, 123.07, 122.56, 121.57, 114.70, 55.48, 48.04, 36.57, 15.93, 15.01.

1,5-Bis(2,5-dimethylthiophen-3-yl)-3-{4-[(4-methylphenyl)(4-methoxyphenyl)amino]phenyl}pentane-1,5-dion e (**3e**). 1.73 g, yellow solid, yield: 57%. m.p. 50-52°C. ^{1}H NMR (400 MHz, $CDCl_3$) δ: (ppm) 7.08-7.02 (m, 8H), 6.92 (dd, J = 11.9, 8.4 Hz, 4H), 6.83 (d, J = 8.8 Hz, 2H), 3.89 (p, J = 6.9 Hz, 1H), 3.81 (s, 3H), 3.16 (ddd, J = 40.8, 16.1, 7.0 Hz, 4H), 2.61 (s, 6H), 2.42 (s, 6H), 2.31 (s, 3H); ^{13}C NMR (100 MHz, $CDCl_3$) δ: (ppm) 194.99, 155.79, 147.21, 146.69, 145.66, 141.06, 136.97, 135.74, 135.01, 131.62, 129.69, 127.96, 126.75, 126.06, 123.52, 122.25, 114.62, 55.48, 48.07, 36.55, 20.75, 15.93, 15.01.

1,5-Bis(2,5-dimethylthiophen-3-yl)-3-{4-(bis[4-methoxyphenyl)amino]phenyl}pentane-1,5-dione (**3f**). 1.49 g, yellow solid, yield: 48%. m.p. 51-53°C. ^{1}H NMR (400 MHz, $CDCl_3$) δ: (ppm) 7.06-7.00 (m, 8H), 6.86 (d, J = 8.3 Hz, 2H), 6.82 (d, J = 8.8 Hz, 4H), 3.87 (p, J = 7.0 Hz, 1H), 3.81 (s, 6H), 3.16 (ddd, J = 40.4, 16.1, 7.0 Hz, 4H), 2.61 (s, 6H), 2.42 (s, 6H); ^{13}C NMR (100 MHz, $CDCl_3$) δ: (ppm) 195.00, 155.55, 147.18, 147.04, 141.28, 136.35, 135.76, 134.99, 127.91, 126.15, 126.07, 121.18, 114.59, 55.49, 48.10, 36.52, 15.91, 14.99.

2.3. Preparation of TPA-DAEs

To a mixture of Zn (60 mmol) and dry THF (80 mL) was added slowly titanium tetrachloride (27 mmol) at 0°C in an atmosphere of argon. The mixture was stirred and refluxed for 2.5 h under argon atmosphere. Subsequently, a solution of corresponding pentane-1,5-dione (1 mmol) in dry THF (30 mL) was added and stirred for 24 h at room temperature in the dark. The reaction mixture was quenched with potassium carbonate solution (10%) and filtered to remove the solid residue. The filtrate was extracted with dichloromethane, washed with brine, dried over magnesium sulphate. After filtration followed by concentration, the crude product was purified by flash column chromatography to afford TPA-DAEs.

N,*N*-diphenyl-4-[3,4-bis(2,5-dimethyl-3-thienyl)-3-cyclopenten-1-yl]benzenamine (**1a**). 1.04 g, white powder, yield: 65%. m.p. 141-142°C. ^{1}H NMR (400 MHz, $CDCl_3$) δ: (ppm) 7.34-7.23 (m, 6H), 7.18-7.00 (m, 8H), 6.52 (s, 2H), 3.66 (p, J = 7.6 Hz, 1H), 3.10 (ddd, J = 20.9, 14.2, 7.7 Hz, 4H), 2.42 (s, 6H), 1.95 (d, J = 8.3 Hz, 6H); ^{13}C NMR (100 MHz, $CDCl_3$) δ: (ppm) 148.04, 145.75, 141.60, 135.18, 135.10, 133.18, 132.47, 129.20, 127.69, 126.04, 124.65, 123.89, 122.43, 46.47, 42.12, 15.25, 14.21. MS (ESI): *m/z* calcd for $C_{35}H_{33}NS_2$: 532.21 $[M+H]^+$; found: 532.76. Elemental analysis calcd. (%) for $C_{35}H_{33}NS_2$: C 79.05, H 6.25, N 2.63; Found C 79.67, H 6.35, N 2.60.

N-phenyl-*N*-(4-methylphenyl)-4-[3,4-bis(2,5-dimethyl-3-thienyl)-3-cyclopenten-1-yl]benzenamine (**1b**). 1.16 g, white powder, yield: 71%. m.p. 108-110°C. ^{1}H NMR (400 MHz, $CDCl_3$) δ: (ppm) 7.28-7.21 (m, 4H), 7.15-7.02 (m, 8H), 6.98 (t, J = 7.3 Hz, 1H), 6.49 (s, 2H), 3.63 (p, J = 7.5 Hz, 1H), 3.07 (ddd, J = 21.0, 14.2, 7.7 Hz, 4H), 2.40 (s, 6H), 2.35 (s, 3H), 1.93 (s, 6H); ^{13}C NMR (100 MHz, $CDCl_3$) δ: (ppm) 148.22, 145.91 145.41, 141.11, 135.14, 135.09, 133.17, 132.48, 132.43, 129.89, 129.07, 127.57, 126.02, 124.71, 124.08, 123.23, 121.89, 46.44, 42.08, 20.85, 15.21, 14.16. MS (ESI): *m/z* calcd for $C_{36}H_{35}NS_2$: 546.23 $[M+H]^+$; found: 546.23. Elemental analysis calcd. (%) for $C_{36}H_{35}NS_2$: C 79.22, H 6.46, N 2.57; Found C 79.74, H 6.54, N 2.54.

N,*N*-bis(4-methylphenyl)-4-[3,4-bis(2,5-dimethyl-3-thienyl)-3-cyclopenten-1-yl]benzenamine (**1c**). 1.11 g, white powder, yield: 66%. m.p. 147-147.5°C. ^{1}H NMR (400 MHz, $CDCl_3$) δ: (ppm) 7.24-7.21 (m, 2H), 7.13-6.99 (m, 10H), 6.50 (s, 2H), 3.63 (s, 1H), 3.08 (ddd, *J* = 17.4, 14.0, 6.1 Hz, 4H), 2.41 (s, 6H), 2.35 (s, 6H), 1.95 (s, 6H); ^{13}C NMR (100 MHz, $CDCl_3$) δ: (ppm) 146.19, 145.67, 140.58, 135.13, 133.21, 132.42, 131.97, 129.80, 127.48, 126.05, 124.16, 123.47, 46.46, 42.10, 20.82, 15.20, 14.16. MS (ESI): *m/z* calcd for $C_{37}H_{37}NS_2$: 559.24 $[M]^+$; found: 559.63. Elemental analysis calcd. (%) for $C_{37}H_{37}NS_2$: C 79.38, H 6.66, N 2.50; Found C 80.17, H 6.73, N 2.47.

N-phenyl-*N*-(4-methoxyphenyl)-4-[3,4-bis(2,5-dimethyl-3-thienyl)-3-cyclopenten-1-yl]benzenamine (**1d**). 1.14 g, white powder, yield: 68%. m.p. 103-105°C. ^{1}H NMR (400 MHz, $CDCl_3$) δ: (ppm) 7.26-7.20 (m, 4H), 7.16-7.09 (m, 2H), 7.08-7.01 (m, 4H), 6.98-6.94 (m, 1H), 6.92-6.84 (m, 2H), 6.49 (s, 2H), 3.84 (s, 3H), 3.65-3.59 (m, 1H), 3.07 (ddd, *J* = 23.0, 15.4, 8.7 Hz, 4H), 2.39 (s, 6H), 1.93 (s, 6H); ^{13}C NMR (100 MHz, $CDCl_3$) δ: (ppm) 156.03, 146.07, 140.95, 140.74, 135.14, 133.18, 132.43, 129.04, 127.54, 127.14, 126.03, 123.43, 122.38, 121.44, 114.74, 55.50, 46.46, 42.07, 15.22, 14.17. MS (ESI): *m/z* calcd for $C_{36}H_{35}NS_2$: 562.22 $[M+H]^+$; found: 562.24. Elemental analysis calcd. (%) for $C_{36}H_{35}NS_2$: C 76.96, H 6.28, N 2.49; Found C 76.27, H 6.36, N 2.47.

N-(4-methylphenyl)-*N*-(4-methoxyphenyl)-4-[3,4-bis(2,5-dimethyl-3-thienyl)-3-cyclopenten-1-yl]benzenamine (**1e**). 0.85 g, white powder, yield: 49%. m.p. 120-120.5 °C. ^{1}H NMR (400 MHz, $CDCl_3$) δ: (ppm) 7.22 (d, *J* = 8.3 Hz, 2H), 7.10 (t, *J* = 9.0 Hz, 4H), 7.01 (d, *J* = 8.2 Hz, 4H), 6.87 (d, *J* = 8.8 Hz, 2H), 6.50 (s, 2H), 3.84 (s, 3H), 3.63 (p, *J* = 7.5 Hz, 1H), 3.07 (ddd, *J* = 21.2, 14.4, 7.7 Hz, 4H), 2.41 (s, 6H), 2.35 (s, 3H), 1.95 (s, 6H); ^{13}C NMR (100 MHz, $CDCl_3$) δ: (ppm) 155.76, 146.42, 145.86, 141.25, 140.07, 135.14, 133.21, 132.42, 131.51, 129.75, 127.44, 126.70, 126.05, 123.41, 122.62, 114.67, 55.51, 46.48, 42.08, 20.80, 15.24, 14.18. MS (ESI): *m/z* calcd for $C_{37}H_{37}NOS_2$: 575.23 $[M]^+$; found: 575.62. Elemental analysis calcd. (%) for $C_{37}H_{37}NOS_2$: C 77.18, H 6.48, N 2.43; Found C 77.79, H 6.54, N 2.40.

N,*N*-bis(4-methoxyphenyl)-4-[3,4-bis(2,5-dimethyl-3-thienyl)-3-cyclopenten-1-yl]benzenamine (**1f**). 1.58 g, white powder, yield: 89%. m.p. 100-102°C. ^{1}H NMR (400 MHz, $CDCl_3$) δ: (ppm) 7.18 (d, *J* = 8.4 Hz, 2H), 7.07 (d, *J* = 8.9 Hz, 4H), 6.94 (d, *J* = 8.4 Hz, 2H), 6.84 (d, *J* = 8.9 Hz, 4H), 6.47 (s, 2H), 3.82 (s, 6H), 3.60 (p, *J* = 8.1 Hz, 1H), 3.04 (ddd, *J* = 21.2, 14.3, 7.8 Hz, 4H), 2.39 (s, 6H), 1.92 (s, 6H); ^{13}C NMR (100 MHz, $CDCl_3$) δ: (ppm) 155.47, 146.74, 141.45, 139.40, 135.14, 135.10, 133.19, 132.38, 127.36, 126.04, 121.51, 114.60, 55.51, 46.45, 42.03, 15.20, 14.15. MS (ESI): *m/z* calcd for $C_{37}H_{37}NO_2S_2$: 591.23 $[M]^+$; found: 591.42. Elemental analysis calcd. (%) for $C_{37}H_{37}NO_2S_2$: C 75.09, H 6.30, N 2.37; Found C 75.68, H 6.37, N 2.34.

3. Results and Discussion

3.1. Synthesis

A series of novel TPA-DAEs were readily obtained by McMurry reaction of **3a~3f** in the presence of the Ti^0 catalyst with yields ranging from 49% to 89%. Two kinds of substituents, methyl and methoxyl group, were introduced into TPA unit. The TPA-DAEs were fully characterized with ^{1}H NMR, ^{13}C NMR and mass spectra.

3.2. Electrochromic devices construction

Electrochromic device based on TPA-DAEs embedded in a sandwich matrix had been prepared by following process. TPA-DAE (0.025 g) and PMMA (0.05 g) were dissolved in dichloromethane (2 mL) with ultrasonic treatment at room temperature. ITO-coated glass slides were washed subsequently with water, acetone, isopropanol, then dried with nitrogen stream. The above solution thinly were spread onto the ITO glass (3 cm × 4 cm) and then dried to form thin films as electrochromic layer. PMMA/$LiClO_4$ polymer electrolyte (PE) and propylene carbonate (PC) were dissolved in dichloromethane and thinly spread onto the aluminum plate, then dried to form thin films as ionic conductive layer.[14] The assembled electrochromic device of ITO glass|TPA-DAE+PMMA|PE|Al|glass was shown in Fig. 1.

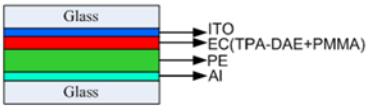

Fig. 1. Structure of electrochromic device.

3.3. Thermal properties

Long term durability is essential to devices based on organic photochromic and electrochromic materials. Herein, the thermal properties of TPA-DAEs were investigated by TG techniques. Typical TG and TGA curves of **1f** in air atmospheres are shown in Fig. 2. The decomposition temperature (T_d) at a 10% weight loss of **1a~1f** in air was recorded at 294, 300, 307, 331, 332, and 374 ^oC, respectively. The results reveal that these TPA-DAEs exhibited good thermal stability.

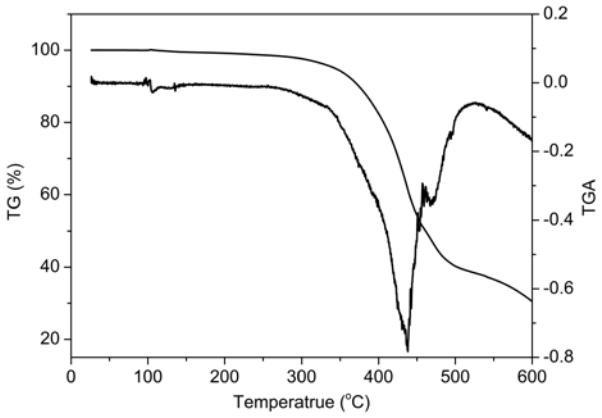

Fig. 2. TG and TGA curves of **1f** with heating rate of 10 ^oC min^{-1}.

3.4. Photochromic properties

TPA-DAEs **1a~1f** showed good photochromism, which could be toggled between the colorless open-ring isomers and the colored closed-ring isomers by alternating irradiation with UV light (302 nm) and blue light (450 nm) in hexane solution and PMMA film. The photochromic process of the diarylethenes is illustrated in Scheme 2.

The photochromic properties of **1a~1f** were measured at room temperature both in hexane (2.0×10^{-5} mol L^{-1}) and in PMMA amorphous films (10%, w/w). Fig. 3 shows the changes in the absorption spectra of **1a** in hexane, which is induced by alternating irradiation with UV and blue light. As shown in Fig. 3, compound **1a** exhibited a

sharp absorption peak at 300 nm in hexane, as a result of a $\pi \rightarrow \pi^*$ transition.[15] Upon irradiation with 302 nm light, the maximum absorption wavelength showed a red shift and increased strength, and also a new visible absorption centered at 445 nm emerged, indicating the formation of the closed-ring isomer. These changes in absorption ware accompanied by the variation of the solution from colorless to yellow. The photostationary state (PSS) was achieved upon irradiation with 302 nm UV light for 20 s.

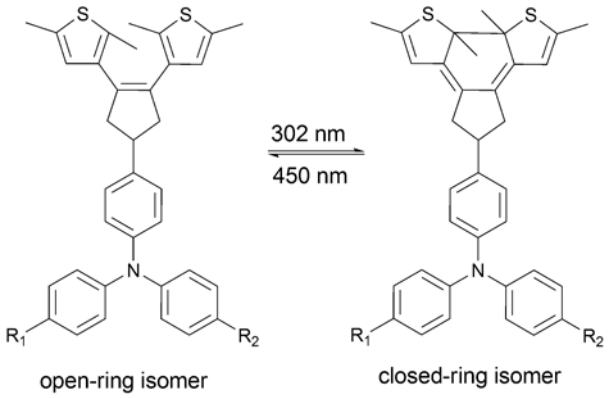

Scheme 2. Photochromism of TPA-DAEs.

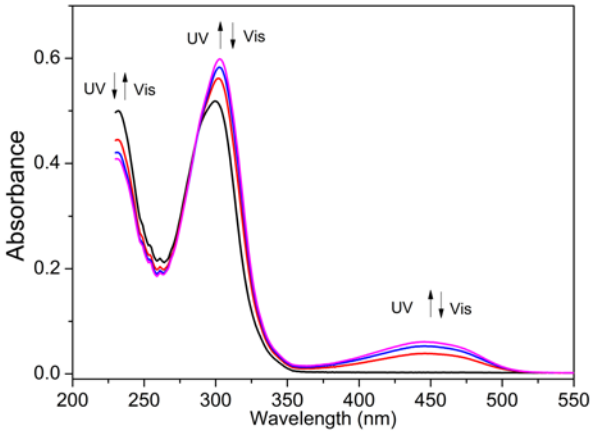

Fig. 3. UV-vis absorption spectral of **1a** upon alternating irradiation with UV (302 nm) and blue light (450 nm) in hexane (2.0×10^{-5} mol L^{-1}) at room temperature.

More significantly, the yellow solution could be bleached completely to colorless upon irradiation with blue light (450 nm) for 30 s, which indicated that the closed-ring isomer returned to the open-ring isomer. Similar to **1a**, compounds **1b~1f** also showed excellent photochromism in hexane. Upon irradiation with 302 nm UV light, absorption bands appeared in the visible region and the hexane solutions of **1b~1f** turned yellow due to cyclization reactions leading to the formation of the closed-ring isomers. The maximum absorption wavelengths were observed at 444, 446, 445, 445, and 447 nm for **1b~1f**, respectively. Alternatively, the yellow colored solution could be bleached completely to colorless upon irradiation with visible light (450 nm), indicating that they returned to the initial state. The absorption spectral features of **1a~1f** were summarized in Table 1. The results showed that the different substituent of TPA had little effect on the photochromism of TPA-DAEs **1a~1f**. The cyclization and cycloreversion quantum yields were determined by comparing the reaction yields of TPA-DAEs

1a~1f against 1,2-bis(2-methyl-5-phenyl-3-thienyl)perfluorocyclopentene in hexane at room temperature,[16] and the results are also listed in Table 1. The results showed that the cyclization quantum yields of **1a~1f** were about 0.15, while the cycloreversion quantum yields were in the range of 0.07~0.18.

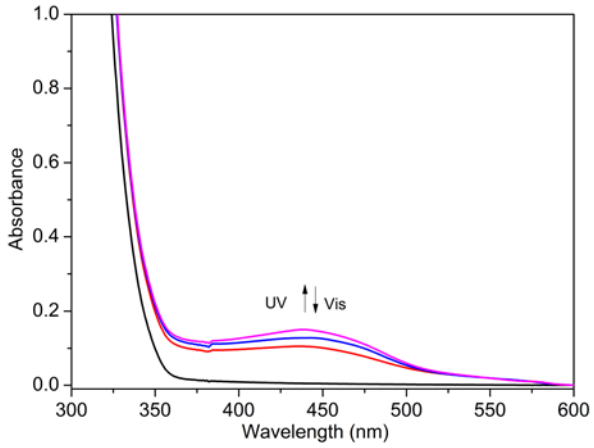

Fig. 4. UV-vis absorption spectral of **1a** upon alternating irradiation with UV (302 nm) and blue light (450 nm) in PMMA film (10%, w/w) at room temperature.

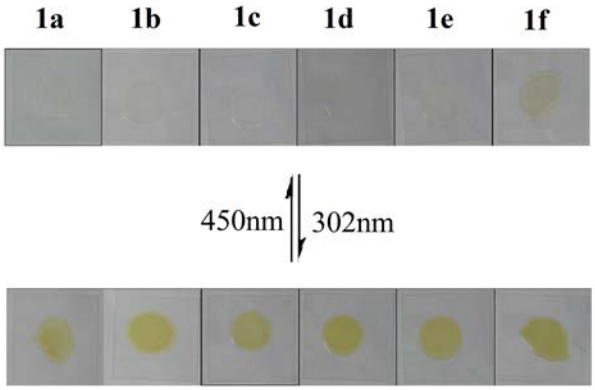

Fig. 5. Color of **1a~1f** upon alternating irradiation with UV (302 nm) and blue light (450 nm) in PMMA film (10%, w/w) at room temperature.

Films were prepared by dissolving TPA-DAE sample (10 mg) and PMMA (100 mg) in chloroform (1.0 mL) with ultrasonication, followed by spin-coating of the solution on the surface of glass substrate. The film thickness of **1a~1f** was 14, 19, 13, 8, 16, and 18 μm, respectively. In PMMA amorphous film, TPA-DAEs **1a~1f** also showed good photochromism. By alternating irradiation with UV and blue light, the representative absorption spectral change of TPA-DAEs in PMMA film was shown in Fig. 4 and the data for **1a~1f** was also listed in Table 1. The color changes of **1a~1f** in PMMA films were shown in Fig. 5. Upon irradiation with 302 nm light, the color of the TPA-DAE/PMMA films changed from colorless to yellow, with the appearance of a new broad visible absorption band centered at 440 nm, which was assigned to the formation of the closed-ring isomers. The colored TPA-DAE/PMMA films can revert to colorless upon irradiation with 450 nm blue light. It is very important for

practical applications of optical devices that photochromic compounds can maintain excellent photochromism property in polymer film.[17]

Table 1 Absorption characteristics and photochromic reactivity of **1a~1f** in hexane (2.0×10^{-5} mol L^{-1}) and in PMMA film (10%,w/w).

Compound	$\lambda_{O,max}$(nm) (ε/L mol^{-1} cm^{-1})	$\lambda_{C,max}$(nm) (ε/L mol^{-1} cm^{-1})		Φ	
	Hexane	Hexane	PMMA film	Φ_{O-C}	Φ_{C-O}
1a	300(5.18×10^4)	445(6.08×10^3)	440	0.15	0.18
1b	301(3.84×10^4)	444(4.53×10^3)	448	0.15	0.07
1c	302(5.21×10^4)	446(5.73×10^3)	448	0.15	0.09
1d	297(6.41×10^4)	445(7.27×10^3)	447	0.12	0.09
1e	299(6.19×10^4)	445(7.25×10^3)	448	0.13	0.16
1f	296(4.25×10^4)	447(5.03×10^3)	440	0.12	0.11

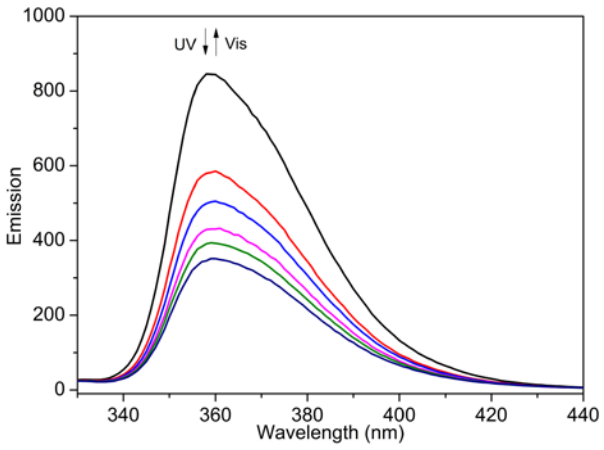

Fig. 6. Fluorescence spectra of **1a~1f** in hexane (2.0×10^{-5} mol L^{-1}) upon irradiation with 302 nm UV light at room temperature.

3.5. Fluorescent properties

Fluorescent properties can be useful not only in molecular-scale optoelectronics,[18] but also for digital photoswitching of fluorescence.[19] The fluorescence modulation is a particularly intriguing approach due to the stabilization of diarylethene and versatility in materials selection.[20] TPA-DAEs **1a~1f** exhibited a very good fluorescent switch on changing from the open-ring isomers to the closed-ring isomers by photoirradiation in hexane. The photoluminescence spectra of **1a** at room temperature are illustrated in Fig. 6. When excited at 300 nm, the emission peaks of TPA-DAEs **1a~1f** were observed at 358, 364, 367, 373, 375, and 384 nm in hexane. Upon irradiation with 302 nm UV light, the photocyclization reaction occurred，hence the emission intensity of TPA-DAEs decreased significantly due to the production of non-fluorescence closed-ring isomers. The fluorescence of the open-ring isomers is quenched on account of the partial overlap between the absorption of

closed-ring isomers and the emission of open-ring isomers. Under irradiation of the 450 nm blue light, the open-ring isomer regenerated and duplicated the original emission spectra. When arriving at the PSS, the emission intensity of TPA-DAE **1a~1f** was quenched to ca. 42%, 42%, 39%, 37%, 36%, and 41%, respectively. The results showed that TPA-DAEs **1a~1f** possessed high fluorescent modulation efficiencies and could be potentially applied to optical memory with fluorescence readout method and fluorescence modulation switches.[21]

3.6. Electrochemical properties

The electrochemical behavior of TPA-DAEs was investigated by cyclic voltammetry (CV) with a conventional three-electrode system. Both working electrode and counter electrode are the platinum plate with a purity of 99.99% respectively, and a saturated calomel electrode (SCE) is used as reference electrode. The electrolyte was dichloromethane containing 0.1 mol L^{-1} Bu_4PF_6 and 1.0×10^{-3} mol L^{-1} TPA-DAE sample. The CV curves of **1a~1f** are shown in Fig. 7. It can be seen from the Fig. 7 that two oxidation peaks appeared at the potential of 1.01 V (E_{pa}^{ox1}) and 1.33 V (E_{pa}^{ox2}) during the positive scan for **1a**. The first oxidation peak can be ascribed to the formation of TPA radical cations, and the second one is attributed to the DAE oxidation. So it was also observed that the color of solution near the working electrode change to blue at the potential of 1.01 V, corresponding to the first oxidation. When the potential is further increased to 1.33 V, the blue color became deeper because of the second oxidation. However, the oxidized TPA-DAE could not be recovered at 1.33V. The two oxidation peaks of **1a** are separated by about 320 mV, so it is possible that DAE moiety would not be affected when TPA moiety is oxidized and reduced at appropriate potential. Similar to **1a**, the CV curves of **1b~1c** also have a couple of reversible redox peaks and an irreversible oxidation peak. However, the third oxidation peak is observed in the CV curves of **1d~1f**, which could be attributed to oxidation of the methoxyl groups.[22] The first two oxidation peaks of **1b~1f** are separated by 390, 460, 510, 550, and 580 mV, respectively. The results show that the distance of first two oxidation peaks could be enlarged when TPA moiety bears electron donating substituent.

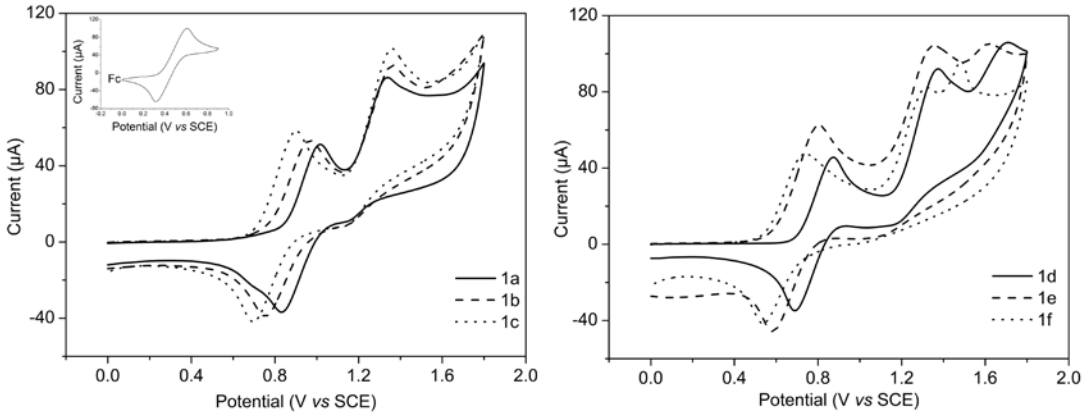

Fig. 7. CV curves of **1a~1f** and ferrocene in dichloromethane (1.0×10^{-3} mol L^{-1}) with a platinum button working electrode at a scan rate of 100mV s^{-1}.

Since ITO glass was often used as anode in electrochromic devices, ITO glass (0.5 mm^2) was used as the working electrode instead of the platinum electrode in the CV experiment. As shown in Fig. 8, a reversible oxidation redox couple and an irreversible oxidation peak are observed for **1a~1f**. The two oxidation peaks of **1a~1f** are separated by 440, 760, 780, 620, 810, and 730 mV, respectively. The potential difference is larger than that of the platinum working electrode, so it is hopeful that ITO glass is used as the anode of electrochromic devices.

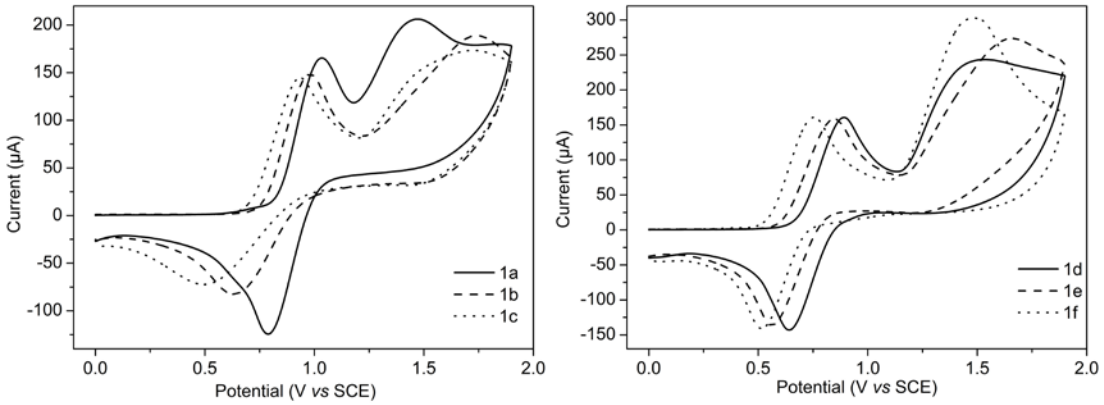

Fig. 8. CV curves of **1a~1f** and ferrocene in dichloromethane (1.0×10^{-3} mol L^{-1}) with a ITO glass (0.5 cm^2) working electrode at a scan rate of 100mV s^{-1}.

The highest occupied molecular orbital (HOMO) energy levels of the investigated TPA-DAEs were calculated from the oxidation onset potentials (E_{onset}) and by comparison with ferrocene (4.8 eV). The lowest unoccupied molecular orbital (LUMO) energy levels were calculated from the HOMO levels with absorption spectra. The results were listed in Table 2. According to the HOMO and LUMO energy levels obtained, **1a~1f** appear to be promising as hole injection and transport materials.[23]

Table 2 Electrochemical properties of **1a~1f**.

Compound	E_{onset} (V)	E_{pa}^{ox1} (V)	E_{pa}^{ox2} (V)	E_{pa}^{ox3} (V)	E_g (eV)[a]	HOMO (eV)[b]	LUMO (eV)[c]
1a	0.80	1.01	1.33	–	2.94	5.24	2.30
1b	0.71	0.97	1.36	–	2.93	5.15	2.22
1c	0.70	0.90	1.36	–	2.87	5.14	2.27
1d	0.70	0.87	1.38	1.71	2.80	5.14	2.34
1e	0.57	0.80	1.35	1.62	2.74	5.01	2.27
1f	0.53	0.74	1.32	1.48	2.69	4.97	2.28

[a] Optical energy gap, $E_g=1240/\lambda_{onset}$ of TPA-DAEs in dichloromethane (2.0×10^{-5} mol L^{-1}). [b] The HOMO energy levels were calculated from E_{onset} and were referenced to ferrocene (4.8 eV). [c] $E_{LUMO}(eV)=E_{HOMO}-E_g$.

For obtaining the excitation voltage of electrochromism, CV curves of electrochromic devices were measured and the cathode was used as the counter electrode and reference electrode. As shown in Fig. 9, the potentials of the first oxidation peaks are 4.38, 4.40, 4.44, 4.17, 4.19, and 3.63 V for **1a~1f**, respectively. The reduction potentials of **1a~1f** are -0.10, -0.41, -0.28, -0.33, -0.39, and -0.02 V, respectively. It is obvious that the first oxidation

potentials would be increased as methyl group was introduced into TPA, and it would change in the opposite trend while the substituent was methoxyl group.

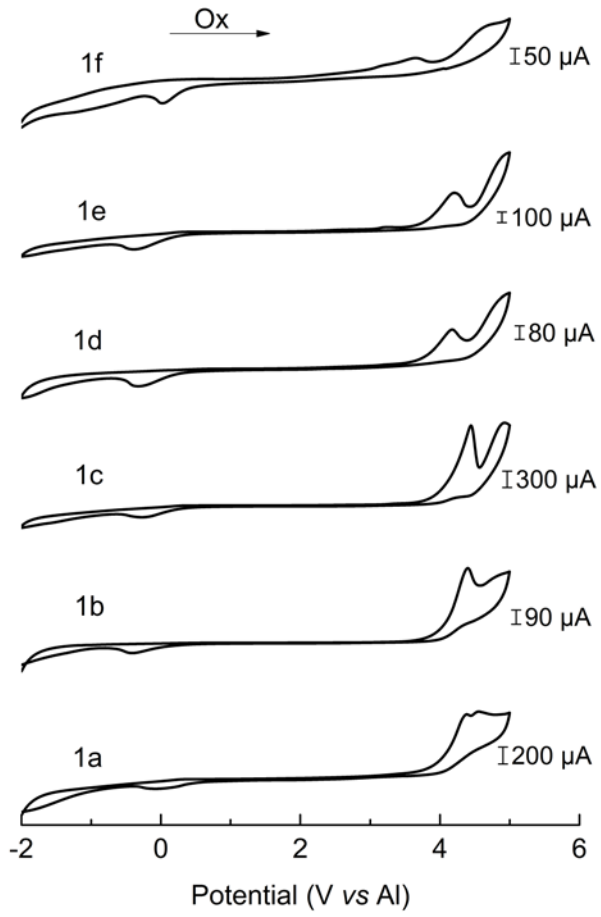

Fig. 9. CV curves of electrochromic devices based on **1a~1f** with a two-electrode configuration at a scan rate of 100mV s^{-1}.

For describing the general features of electrochromic devices and further identifying the underlying electrochromic mechanism, electrochemical impedance spectroscopy (EIS) was investigated. Fig. 10 shows Nyquist plots of electrochromic devices based on **1a~1f**. These plots are complex plane representations of the imaginary part of the impedance response, reactance or Z″, and the real part of the impedance, resistance or Z′. In the several Nyquist plots, they may be lines with different slopes at the low frequency domain, because EC layer including PMMA is passivated and results in tremendously high resistivity and suppressed cation transporting. The internal impedances were determined by fitting the experimental data with an equivalent circuit, R(CR)(CR) (Fig. 10, inset), which consist of a resistor R_s in series with two resistors R_1, R_2 and capacitors C_1, C_2 in parallel respectively. The R_s circuit element represents resistive losses in the PE layer, R_1 and C_1 represent the response of anode and EC layer, R_2 and C_2 represent the response of cathode. Fitting results determined from EIS analysis are listed in Table 3. C_1 of the devices based on TPA-DAEs are 7.549, 5.059, 7.053, 4.483, 4.939, and 6.755 μF, respectively, which could show the oxidation degree of EC layer.

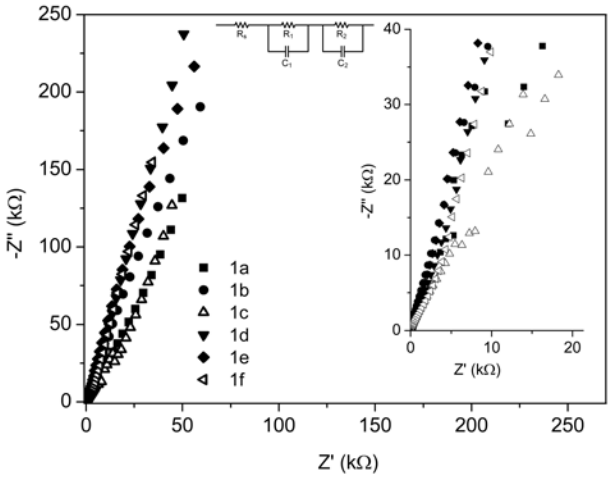

Fig. 10. Nyquist plots of electrochromic devices based on **1a~1f**. Inset shows the equivalent circuit.

Table 3 Fitting results of **1a~1f** determined from EIS analysis.

Compound	R_s(Ω)	R_1(KΩ)	C_1(μF)	R_2(KΩ)	C_2(μF)
1a	36.16	584.9	7.549	1.110	6.118
1b	57.14	482.9	5.059	2.709	4.264
1c	63.02	321.3	7.053	5.356	4.268
1d	57.44	765.3	4.483	3.617	2.585
1e	42.75	648.2	4.939	2.481	3.755
1f	46.51	484.7	6.755	3.048	2.399

3.7. Spectroelectrochemical and electrochromic properties

Spectroelectrochemistry is the best way of examining the changes in optical properties of electrochromic material upon voltage applied. The spectroelectrochemical and electrochromic properties of electrochromic devices based on resultant six TPA-DAEs were studied with a self-established system for measuring reflection spectra (Supporting Information, Fig. S1) by applying stepped potentials sequentially. In this system, the reflectance minimum is just about the absorption maximum because the light that could not be absorbed by TPA-DAEs would all be reflected into prober. The potential of the first oxidation peak is adopted as the electrochromism voltage, recover voltage is -0.5 V, which is so lower than that of CV curves hence the color could be recover quickly. The electrochromism and recover voltage were all applied in 16 s. To more completely understand the changes occurring in the visible region，the reflection spectra of **1a~1f** were measured. Fig. 11 showed the reflection spectra of **1a**. In the coloring process, reflectance at 763.3 nm tended to decrease with time, and it would increase to initial level in the recover process, then a spoon was formed. As same as **1a**, the reflection spectra of **1b~1f** with time would form spoons, too. The reflection spectra of **1a~1f** after coloring were shown in Fig. 12. The reflectance minima of **1b~1f** are found at around 781.7, 709.7, 726.9, 723.9, and 741.8 nm, respectively. While the light band comes near 780 nm, the boundary of visible light, response of eyes would be weakening. It is clear that **1c** is the most excellent electrochromic materials in the six compounds.

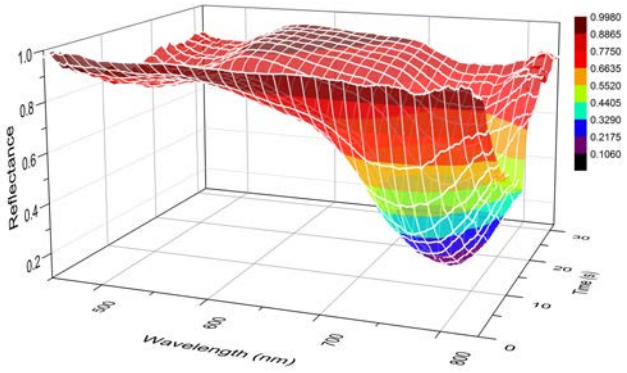

Fig. 11. 3D spectroelectrochemical behavior of electrochromic devices based on **1a**. 4.38 V was applied from 0 s to 16 s, -0.5 V was applied from 17 s to 32 s.

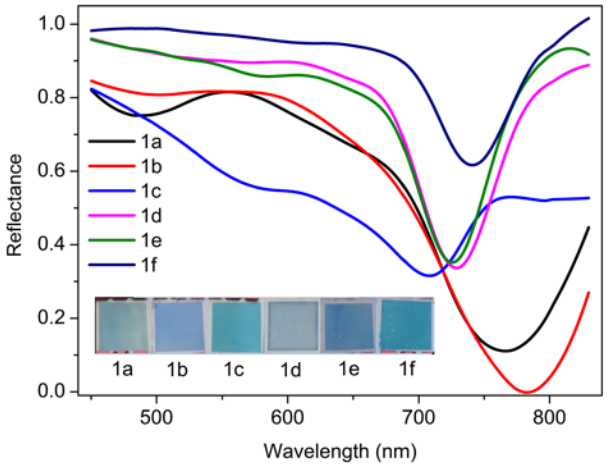

Fig. 12. Reflection spectra of electrochromic devices based on **1a**~**1f** after coloring.

For electrochromic switching studies, chronoamperometric and reflectance measurements were performed. While the electrochromic devices of **1a~1f** were switched, the reflectance was monitored as a function of time with visible spectroscopy at the corresponding reflectance minima. Optical switching data were shown in Fig. 13. The switching time was calculated at 90% of the full switch because it is difficult to perceive any further color change with naked eye beyond this point. The electrochromic devices of **1a~1f** require 8.6~12.1 s for color switching and 8.9~12.8 s for bleaching. Comparing the electrochromic data, the color switching times of **1a~1f** are somewhat slower than the typical switching time of 1~2 s for TPA polymer films, and the bleaching times are slower about 10 s.[24] This may be due to slow ion permeation or relatively high internal resistance caused by PMMA. For **1a**, **1b** and **1d**, reflectance would be reduced by 47%, 43% and 38% after five cycles due to electropolymerization. Although the side reaction also exists for poly(amine–amide)s with pendent TPA moieties,[25] it can be controlled effectively because of the less contact between the two TPA unites attached to polymer chain. As for small molecules **1a**, **1b** and **1d**, the side reaction is cannot be suppressed effectively hence results in less stable electrochromic properties compared to that of polymer. While, as shown in Fig. 13, **1c**, **1e** and **1f** show excellent electrochromic stability, which is comparable to that of aromatic polyamides containing pendent

dimethyltriphenylamine moieties,[26] The high electrochromic stability of **1c**, **1e** and **1f** could be explanation by the reason that the replacement of all the *p*-position hydrogen atoms on the benzene ring of TPA by methyl or methoxyl group could prohibit the electropolymerization. Therefore, the results revealed that TPA-DAEs, especially **1c**, could be a good candidate as anodic electrochromic materials.

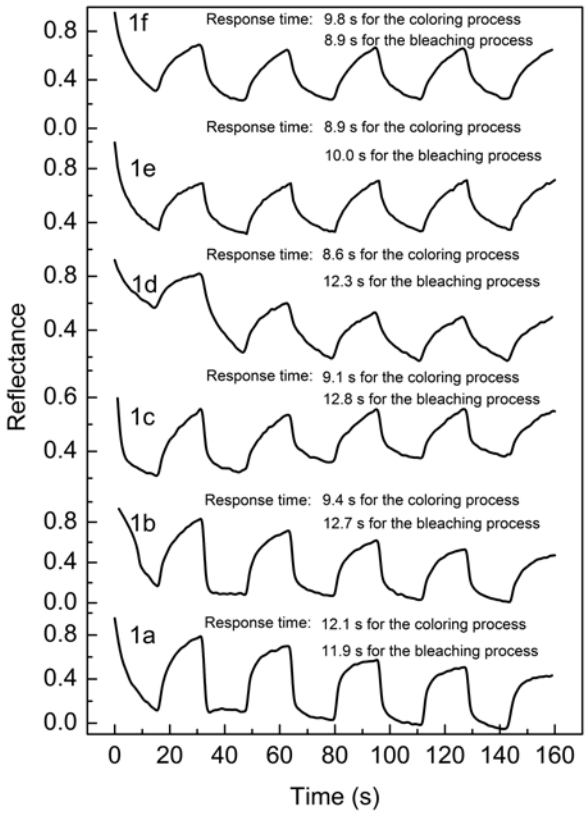

Fig. 13. Electrochromic switching and reflectance change monitored at reflectance minima for electrochromic devices based on **1a**~**1f**.

4. Conclusion

In the present work, six novel photochromic and electrochromic compounds containing diarylethene and triphenylamine units have been successfully synthesized and characterized. The photochromic, electrochromic, electrochemical and fluorescent properties were investigated in detail. All of these compounds showed good photochromism both in solution and PMMA film, and acted as a remarkable fluorescent switch. The electrochromic devices based on TPA-DAEs were fabricated and investigated by CV and EIS analysis. The CV curves of electrochromic devices showed that the oxidation potentials would be increased if methyl group was introduced into TPA; nevertheless, it would be decreased when the substituent was methoxyl group. Spectroelectrochemical and electrochromic switching properties were investigated. TPA-DAEs exhibit excellent electrochromic behavior, with coloration change from colorless to blue. Thus, TPA-DAEs could be good candidates as anodically electrochromic materials due to their proper oxidation potentials and good electrochemical stability. The reflectance minimum of **1c** with two methyl groups is found at 709.7 nm, which is

an excellent electrochromic material. The results will be helpful for designing materials, which respond to both light and electronic dual control.

Acknowledgments

This work was financially supported by the National Natural Science Foundation of China (Grant no. 21102098) and the Key Technology R&D Program of Tianjin (Grant no. 11ZCKFGX01700).

References

1 Z. Y. Li, J. Yin, X. H. Wu, Y. Lin, Q. B. Zeng, F. Y. Fan and S. H. Liu, *J. Photoch. Photobio. A*, 2011, **218**, 192.

2 Z. Niu and H. W. Gibson, *Chem. Rev.*, 2009, **109**, 6024.

3 (a) F. Terao, M. Morimoto and M. Irie, *Angew. Chem. Int. E.*, 2012, **51**, 901; (b) R. J. Wang, S. Z. Pu, G. Liu, S. Q. Cui and W. J. Liu, *Tetrahedron Lett.*, 2012, **53**, 320.

4 (a) J. J. Zhang, W. J. Tan, X. L. Meng and H. Tian, *J. Mater. Chem*., 2009, **19**, 5726; (b) H. Tian, B. Qin, R. Yao, X. Zhao and S. Yang, *Adv. Mater*., 2003, **15**, 2104.

5 Y. Kutsunugi, C. Coudret, J. C. Micheau and T. Kawai, *Dyes Pigments*, 2012, **92**, 838.

6 (a) H. F. Li, T. Koike and M. Akita, *Dyes Pigments*, 2012, **92**, 854; (b) K. Motoyama, T. Koike and M. Akita, *Chem. Commun*., 2008, **44**, 5812.

7 (a) S. Fukumoto, T. Nakashima and T. Kawai, *Dyes Pigments*, 2012, **92**, 868; (b) H. H. Liu and Y. Chen, *J. Phys. Org. Chem.*, 2012, **25**, 142.

8 C. G. Granqvist, *Sol. Energy Mater. Sol. Cells*, 2000, **60**, 201.

9 Y. Kim, J. Do, E. Kim, G. Clavier, L. Galmiche and P. Audebert, *J. Electroanal. Chem.*, 2009, **632**, 201.

10 G. Sonmez, *Chem. Commun*., 2005, **42**, 5251.

11 D. Corr, U. Bach, D. Fay, M. Kinsella, C. McAtamney, F. Reilly, S. N. Rao and N. Stobie, *Solid State Ionics*, 2003, **165**, 315.

12 F. K. Chen, X. Y. Fu, J. Zhang and X. H. Wan, *Electrochim. Acta*, 2013, **99**, 211.

13 (a) H. J. Yen, H. Y. Lin and G. S. Liou, *Chem. Mater*., 2011, **23**, 1874; (b) C. W. Chang and G. S. Liou, *J. Mater. Chem*., 2008, **18**, 5638.

14 D. J. Yang, X. K. Fu and Y. F. Gong, *Acta Chim. Sin*., 2008, **8**, 975.

15 Z. X. Li, L. Y. Liao, W. Sun, C. Xu, C. Zhang and C. J. Fang, *J. Phys. Chem. C*, 2008, **112**, 5190.

16 M. Irie, T. Lifka, S. Kobatake and N. Kato, *J. Am. Chem. Soc*., 2000, **122**, 4871.

17 S. Z. Pu, C. B. Fan, W. J. Miao and G. Liu, *Tetrahedron*, 2008, **64**, 9464.

18 B. Gorodetsky, H. D. Samachetty, R. L. Donkers, M. S. Workentin and N. R. Branda, *Angew. Chem. Int. Ed*., 2004, **43**, 2812.

19 S. Z. Xiao, T. Yi, Y. F. Zhou, Q. Zhao,F. Y. Li and C. Huang, *Tetrahedron*, 2006, **62**, 10072.

20 (a) C. C. Corredor, Z. L. Huang and K. D. Belfield, *Adv. Mater*., 2006, **18**, 2910; (b) S. Z. Pu, H. Li, G. Liu, W. J. Liu, S. Q. Cui and C. B. Fan, *Tetrahedron*, 2011, **67**, 1438; (c) G. Liu, M. Liu, S. Z. Pu, C. B. Fan and S. Q. Cui, *Dyes Pigments*, 2012, **95**, 553.

21 T. B. Norsten, N. R. Branda, *J. Am. Chem. Soc*., 2001, **123**, 1784.

22 S. H. Hsiao, G. S. Liou, Y. C. Kung and T. J. Hsiung, *J. Polym. Sci. Pol. Chem*., 2010, **48**, 3392.

23 W. Z. Gao, S. R. Wang, Y. Xiao and X. G. Li, *Dyes Pigments*, 2013, **97**, 92.

24 (a) H. J. Yen and G. S. Liou, *Org. Electron*., 2010, **11**, 299; (b) W. H. Chen, K. L. Wang, D. J. Liaw, K. R. Lee and J. Y. Lai, *Macromolecules*, 2010, **43**, 2236.

25 G. S. Liou, S. H. Hsiao and T. H. Su, *J. Mater. Chem*., 2005, **15**, 1812.

26 (a) C. W. Chang, G. S. Liou and S. H. Hsiao, *J. Mater. Chem*., 2007, **17**, 1007; (b) C. W. Chang, S. H. Hsiao and G. S. Liou, *Macromolecules*, 2008, **41**, 8441.